J. Korean Soc. Aeronaut. Space Sci. 49(12), 1019-1025(2021)
DOI:https://doi.org/10.5139/JKSAS.2021.49.12.1019
ISSN 1225-1348(print), 2287-6871(online)

태양 양성자 이벤트에 의한 삼중 접합 GAGET2-ID2 태양전지 열화

구자춘[1], 박정언[2], 문건우[3]

Triple Junction GAGET2-ID2 Solar Cell Degradation by Solar Proton Events

Ja-Chun Koo[1], Jung-Eon Park[2] and Gun-Woo Moon[3]
Korea Aerospace Research Institute[1,2]
Department of Electrical Engineering, Korea Advanced Institute of Science and Technology[3]

ABSTRACT

In nearly all space environments, the solar cell degradation is dominated by protons[1]. Even through a GEO orbit lines in the electron radiation belts, the protons emitted from any solar event will still dominate the degradation[1]. Since COMS launch on June 26 2010, the proton events with the fluence of more than approximately 30 times the average level of perennial observations were observed between January 23 - 29 2012 and March 07 - 14 2012[16]. This paper studies the solar cell degradation by solar proton events in January and March 2012 for the open circuit voltage(Voc) of a witness cell and the short circuit current(Isc) of a section connected to a shunt switch. To evaluate the performance of solar cell, the flight data of voltage and current are corrected to the temperature, the Earth-Sun distance and the Sun angle and then compare with the solar cell characteristics at BOL. The Voc voltage dropped about 23.6mV compare after the March 2012 proton events to before the January 2012 proton events. The Voc voltage dropped less than 1% at BOL, which is 2575mV. The Isc current decreased negligible, as expected, in the March 2012 proton events.

초 록

거의 모든 우주 환경에서 태양전지 열화는 양성자에 의해 좌우된다. 정지궤도는 전자 방사선 벨트에 위치하지만 태양 이벤트에서 방출된 양성자는 여전히 태양전지 열화의 주된 요소이다. 2010년 6월 26일 천리안 1호가 발사된 이후로, 2012년 1월 23일에서 29일 그리고 2012년 3월 7일에서 14일에 다닌 평균 관측 수준의 약 30배 이상의 플루언스를 갖는 양성자 이벤트가 관측되었다. 본 논문은 2012년 1월과 3월에 발생한 태양 양성자 이벤트에 의해 감시 셀의 개방회로 전압(Voc)과 션트 스위치에 연결된 한 섹션의 단락회로 전류(Isc)에 대한 태양전지 열화에 대해 연구한다. 태양전지의 성능을 평가하기 위해 전압과 전류의 비행 데이터는 온도, 지구-태양 거리, 태양 각도로 보정한 후 임무 초기 태양전지 특성과 비교한다. Voc 전압은 2012년 1월 양성자 이벤트 이전과 비교하여 2012년 3월 양성자 이벤트 이후에 약 23.6mV 감소되었다. 감소된 Voc 전압은 임무 초기값 2575mV에 대해 1% 미만이다. Isc 전류는 예상대로 2012년 3월 양성자 이벤트에서 무시할 정도로 감소되었다.

Key Words : Solar Proton Event(태양 양성자 이벤트), Radiation Belts(방사선 벨트), Triple Junction GaAs Solar Cell(삼중 접합 GaAs 태양전지), Degradation(열화)

† Received : September 17, 2021 Revised : November 22, 2021 Accepted : November 26, 2021
[1] Principle Researcher, [2] Senior Researcher, [3] Professor
[1] Corresponding author, E-mail : jckoo@kari.re.kr, ORCID 0000-0002-4008-4320
© 2021 The Korean Society for Aeronautical and Space Sciences

Ⅰ. Introduction

The proton flux is particularly significant in the context of solar cell degradation[2]. Damage accumulates via collisional atomic displacements, referred to as nonionizing dose, leading to a drop in performance and potential shortening of mission lifetime[2]. For electrons, unlike protons, it is the high-energy particles that do more damage per collision, and these fluxes are less affected[2]. Because power decreases logarithmically with dose, an extra contribution from trapped electrons has only a minor effect on the remaining power[2].

Since COMS(Communication, Ocean and Meteorological Satellite) launch on June 26 2010 (UTC), the strongest proton events were observed between January and March 2012. This paper studies the solar cell degradation by solar proton events in January and March 2012 for the Voc voltage of a cell and the Isc current of a section. The Sun-Earth distance and Sun angle on GEO(Geostationary Earth Orbit) varies throughout the year. To evaluate the performance of solar cell, the flight data of the voltage and the current are corrected to the temperature, the Earth-Sun distance and the Sun angle and then compare with the solar cell characteristics at BOL.

Ⅱ. Solar Radiation Environment

2.1 Van Allen Radiation Belts

The Earth's radiation belts are two large and distinct toruses of high energy plasma that surround Earth[3]. The highly stable inner belt is composed mostly of relativistic protons and lies approximately 1.2 to 3 Earth radii away from Earth's surface[3]. The outer belt, located at 4 to 7 Earth radii away from the surface, is compromised of mostly relativistic and ultra relativistic electrons [3]. The outer belt is highly dynamic and sensitive to changes in geomagnetic activity and the solar wind[3]. Fig. 1 shows the radiation belts in context of Earth and GEO[3].

Figure 2 shows a summary of expected annual doses behind 4mm spherical shielding on circular equatorial orbits as a function of the orbit altitude[4]. The effects of the trapped particles are degradation of solar array performance due to displacement damage[5]. Both electrons and protons contribute to the total dose[5]. The major contribution will depend on the particular orbit; in general, low altitude orbits (less than about 800km) will be dominated by protons, whereas high altitude orbits including GEO, will be dominated by electrons[5]. Both types of particles will cause displacement damage, but protons are more effective[5]. The damage influence of an individual massive particle, such as a proton, is significantly greater than that from an electron due to the higher momentum carried by the former[5].

Figure 3 gives an example of the radiation environment that exists for satellites travelling in a GEO after 15 years[6] as a function of the particle energy. The GEO orbit is electron dominated orbit.

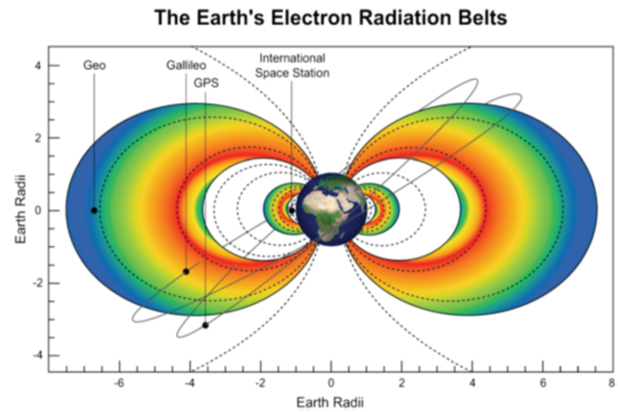

Fig. 1. Earth's radiation inner and outer belts where color serves as a proxy for flux levels[3]

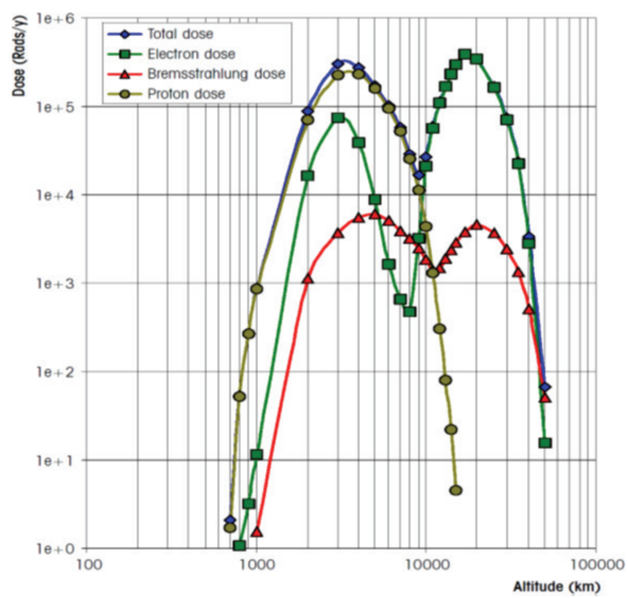

Fig. 2. Annual doses on circular equatorial orbits in the radiation belts[4]

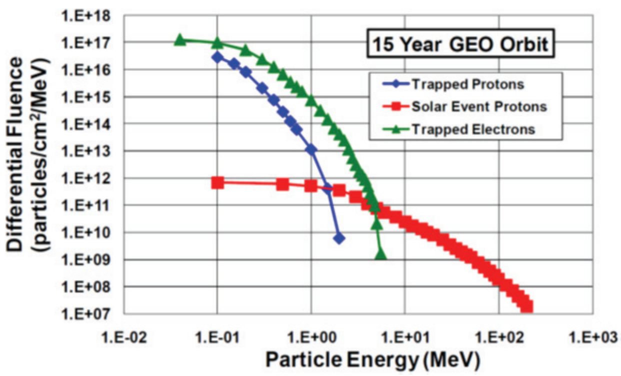

Fig. 3. Particle radiation environment in a GEO after 15 years[6]

2.2 Energetic SPE(Solar Proton Event)s

The Sun sometimes discharge large amount of energetic particles that are hazard to instruments in space[7]. Fig. 4 shows the two-class picture for SPEs. The impulsive event (left) is produced by a solar flare that populates only those IMF (Inter-planetary Magnetic Field) lines well-connected to the flare site[7]. The gradual event (right) is produced by a large-scale CME(Coronal Mass Ejection) driven shock wave that accelerates the solar particles and populates IMF lines over a large longitudinal area[7]. The SPEs occur when protons emitted by the Sun become accelerated either close to the Sun during a flare or in interplanetary space by CME shocks[7]. During a large SPE, the fluence of protons with energies greater than 30MeV can exceed 10^{10}cm^{-2} in several hours or days[7].

2.3 Solar Cycle and SPE Intensity

Figure 5 shows the proton events intensity plotted with the sunspot numbers as a curve of solar activity since 1996. The solar cycle is approximately eleven years in length and contains periods of high activity, known as “solar maximum,” and periods of low activity, known as

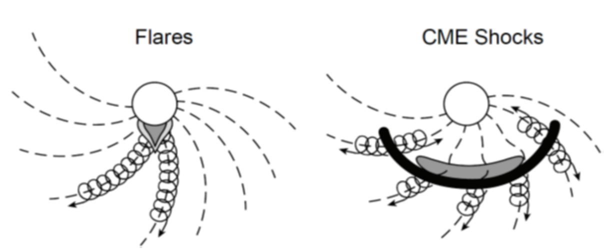

Fig. 4. The two-class picture for SPEs where the impulsive event(left) & the gradual event(right)[7]

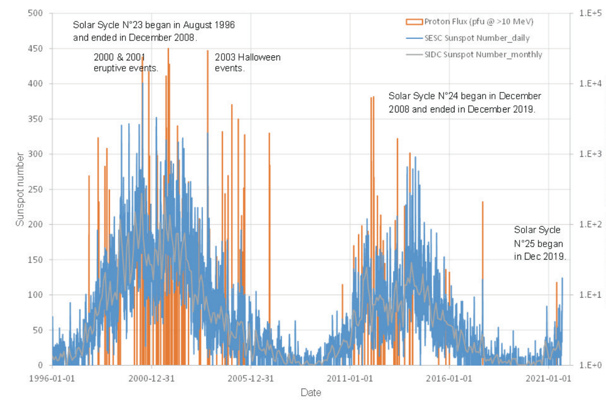

Fig. 5. SPEs intensity with sunspot numbers since 1996

“solar minimum”[8]. During solar maximum, there tend to be more frequent and higher intensity SPEs[8], as is evident in Fig. 5. Daily sunspot numbers are a number of the sunspots observed per a day and data gathered from [9]. Monthly sunspot numbers are a number of the sunspots observed monthly mean values and data gathered from [10]. A significant energetic SPE is proton flux greater than 10MeV intensities above 10 particles cm^{-2}s^{-1}sr^{-1} and data gathered from [9].

2.4 Typical GaAs/Ge Solar Cell Radiation Hardness

Figure 6 shows the degradation of the Pmax from illuminated current-voltage data taken under space solar environmental conditions[12] under AM0 (Air Mass 0), 1 Sun illumination at 25°C for an extensive ground irradiation data set taken on bare (e.g. uncovered) single junction GaAs/Ge solar cells. The data represent normal incidence ground irradiation testing for several mono-energetic electron and proton energies over a wide fluence

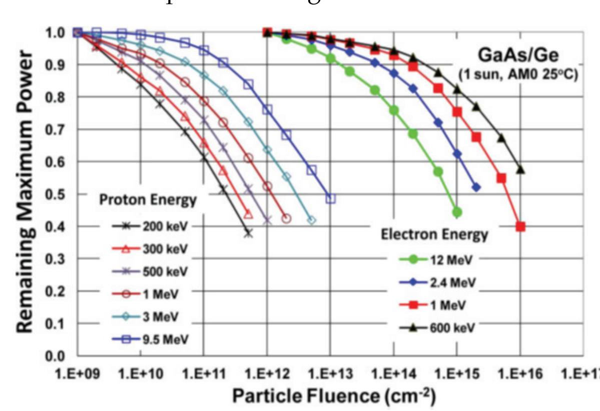

Fig. 6. Ground irradiation data for single junction GaAs/Ge solar cells[12]

range[12]. In the case of electron irradiation, higher energy electrons induce greater radiation damage, whereas in the case of proton irradiation, the opposite is observed[15] (i.e. lower energy protons induce greater radiation damage).

III. COMS GAGET2-ID2 Solar Cell Degradation by SPEs in 2012

3.1 COMS Solar Array Configuration

Figure 7 shows the COMS solar array wing configuration. The solar array wing is divided into 8 sections including 7 main sections and 1 battery charge section. The charge section is located on the outer panel. Each panel provides 59 circuits of 28 SCA(Solar Cell Assembly)s in series each. The solar array supports 3304 SCAs in total on 2 panels. The SCA is an assembly of a triple junction GaAs solar cell (dimensions of 40mm x 80mm), a 12.5μm Ag - inter connector and a 100μm thick cover glass (dimensions of 40.15mm x 80.15mm) bonded to the connector integrated cell. The solar cell type is GAGET2-ID2/160-8040, manufactured by the RWE (now AZUR) with integral 2.5V bypass diode protecting the adjacent cell on SCA level. Active solar cell area is 30.18cm^2 due to cropped corners. One set of solar cell life witnesses is implemented on inner panel to monitor the Voc trend along spacecraft in orbit life. Each wing provides two platinum temperature sensors mounted on each panel at rear side.

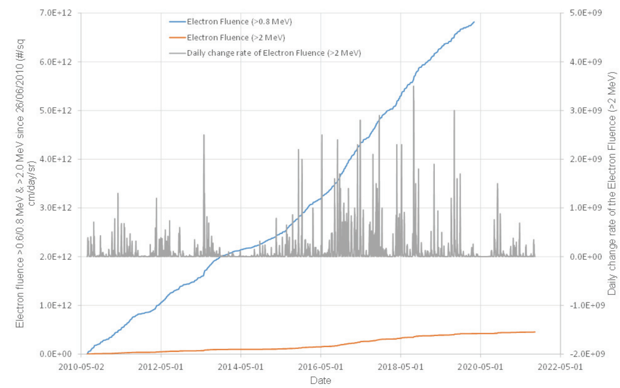

Fig. 8. Electron fluence since COMS launch

3.2 Electron and Proton Fluence since COMS Launch

The COMS launched on June 26 2010 and reached its GEO location on July 4 2010. Fig. 8 and Fig. 9 show the electron fluence and the proton fluence respectively since COMS launch. Daily particle data gathered from the NOAA (National Oceanic and Atmospheric Administration) SWPC(Space Weather Prediction Center)[9,11] are a number of electron and proton flux integral a day. Daily particle data are measured by 3rd generation GOES-N(GOES-13, GOES-14, and GOES-15) series and 4th generation GOES-R(GOES-16) series. Prior GOES-R series sensors had two integral electron channels (>0.8MeV and >2MeV)[13]. The SWPC alerts are based on the >2MeV channel[13]. The GOES-16 and subsequent satellites in the GOES-R series will only have the >2MeV integral channel

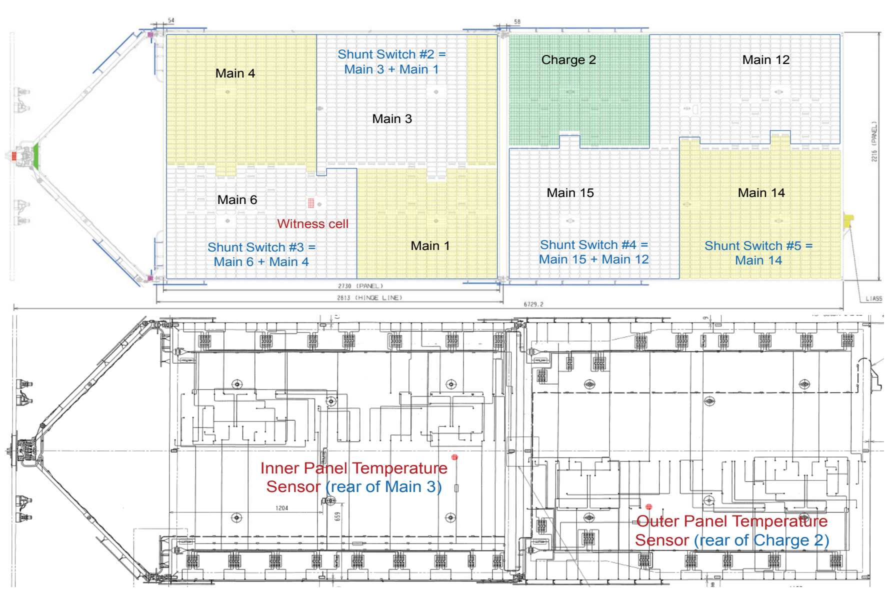

Fig. 7. COMS solar array wing configuration at front side (upper) and at rear side (lower)

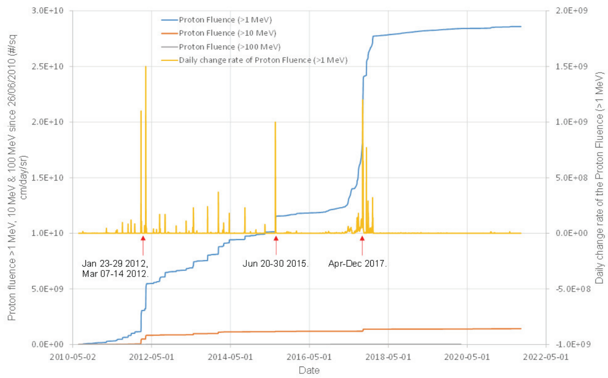

Fig. 9. Proton fluence since COMS launch

[13]. Since COMS launch, the proton event (Fig. 9) were observed between January 23-29 2012, between March 07-14 2012, between June 20-30 2015, and between April and December 2017. The strongest proton events with the fluence of more than approximately 30 times the average level of perennial observations were observed between January 23-29 2012, and between March 07-14 2012 [16]. These fluence can be shown on Fig. 9 by the daily change rate of the proton fluence (>1MeV). Therefore, this paper analyzes the performance degradation of solar cells in the January and March 2012 proton events.

Figure 10 shows the proton fluence and SPEs observed between January and March 2012. The proton fluence is in line with the SPEs. The proton fluence gathered from [9,11] and the SPEs gathered from [9]. The p.f.u. is proton flux unit (1 particle $cm^{-2}s^{-1}sr^{-1}$)[14]. The measurement of proton flux[14] by GOES is reaching and sustaining ~10 p.f.u. for at least 15 minutes at energies >10MeV. The start time of the event is defined as the earliest time at which event thresholds have been reached[14]. The end time is the last time 10 p.f.u.

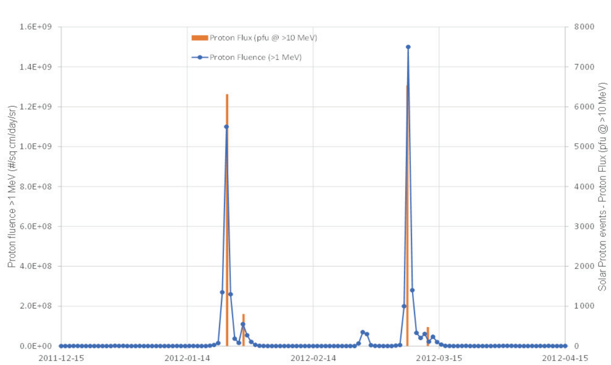

Fig. 10. Proton fluence and SPEs in the January and March 2012

observed[14]. This definition allows multiple injections from flares and interplanetary shocks to be encompassed by a single event[14].

3.3 COMS Flight Data

The COMS flight data are averaged during 5 hours, from UTC 09:00 to 14:00, at each day to remove effects by stopping the wing rotation during GOCI(Geostationary Ocean Color Imager) imaging periods. Fig. 11 shows the witness cell Voc voltage and the shunt switch #5 (allocated to main section #14 in Fig. 7) Isc current during 4 months including proton events at January and March 2012. The Voc voltage dropped at January and March 2012 proton events. But the Isc current decreased negligible at March 2012 proton events.

3.4 COMS Flight Data Corrections

Variation of the Earth-Sun distance does lead to variation of extraterrestrial radiation flux in the range of ±3.3%[17]. The dependence of extraterrestrial radiation on time of year is shown in Fig. 12. The eccentricity correction factor of the Earth's orbit provides a more accurate equation (±0.01%), in the form of Eq. (1)[17]:

$$G_{on} = G_{sc}\begin{pmatrix} 1.000110 + 0.034221 \times \cos(B) \\ + 0.001280 \times \cos(B) + 0.000719 \\ \times \cos(2B) + 0.000077 \times \sin(2B) \end{pmatrix} \qquad (1)$$

where Gsc is the solar constant of $1367Wm^{-2}$ and G_{on} is the extraterrestrial radiation incident on the plane normal to the radiation on the n^{th} day of the year and B is given by Eq. (2)[17]:

$$B = (n-1) \times \frac{360}{365} \qquad (2)$$

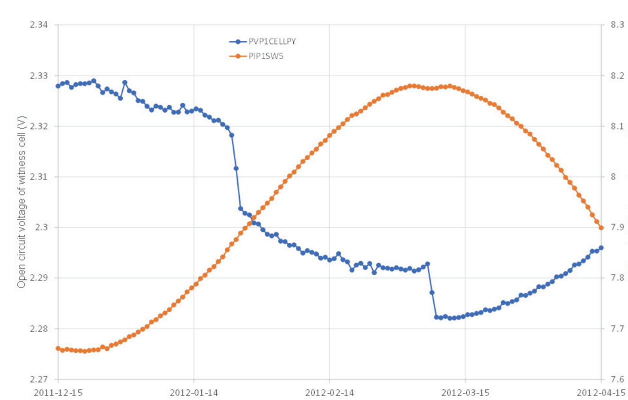

Fig. 11. Witness cell Voc voltage and shunt switch Isc current

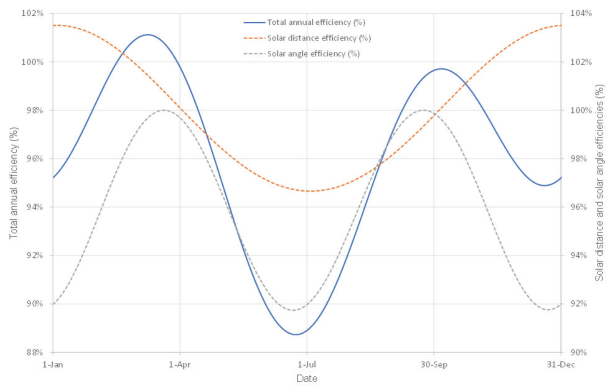

Fig. 12. Solar distance, angle & annual efficiencies

The position of the satellite relative to the Sun varies throughout the year[18]. As the earth goes around its orbit, its distance from the Sun changes from a minimum of 0.983 AUs to a maximum of 1.067 AUs[18]. If we consider the energy received from the Sun at 1 AU to be 100%, then the energy received varies from 97% to 103%[18], as shown in Fig. 12. The declination δ can be found from the more accurate equation (error<0.035°) in the form of Eq. (3)[17]:

$$\delta=\left(\frac{180}{\pi}\right)\times\begin{pmatrix}0.006918-0.399912\times\cos(B)\\+0.070257\times\sin(B)-0.006758\\\times\cos(2B)+0.000907\times\sin(2B)\\-0.002697\times\cos(3B)+0.00148\\\times\sin(3B)\end{pmatrix} \tag{3}$$

where B is from Eq. (2) on the n^{th} day of the year. Variation in Sun-Earth distance and the declination are all continuously varying functions of time of year[17]. If we combine the effects of variations in solar distance and solar angle over the course of a year, we get the result in Fig. 12. Both the solar distance efficiency and the solar angle efficiency are independent. Therefore the solar distance efficiency multiplied by the solar angle efficiency leads to the total annual efficiency as can be seen in Fig. 12. Total solar energy available varies 12% from a low of 89% to a high of 101%[18].

An objective of data processing is to define dependence of degradation on time in flight under AM0 environment. For approximation, the following factors were taken into account luminosity[16]:

- for V_{OC} - only temperature dependence,
- for I_{SC} - temperature dependence, direct dependence on illumination level.

To evaluate the performance of solar cell, we can correct the COMS flight data, the witness cell Voc voltage and the shunt switch #5 Isc current, to compare with datasheets (1 Sun, AM0, 28°C) from RWE. The flight temperature data from the inner panel and the outer panel, each sensor location as shown in Fig. 7, were used to correct the Voc voltage and the Isc current respectively.

Figure 13 shows the witness cell Voc voltage after only temperature correction. The Voc voltage difference is about 23.6mV compare before the January 2012 proton events to after the March 2012 proton events. The Voc voltage dropped less than 1% of the datasheets (2575mV at BOL). Fig. 14 shows the shunt switch #5 Isc current after corrections of the temperature, the Earth-Sun distance and the Sun angle. The Isc current decreased negligible, as expected, at March 2012 proton events. The temperature is a small effect to correct current. Both the Earth-Sun distance and the Sun angle are major effect to correct current.

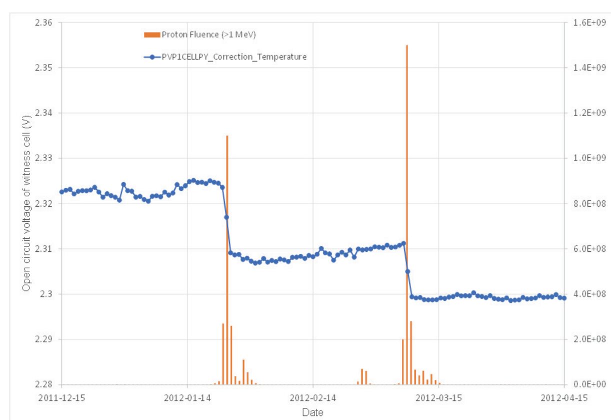

Fig. 13. Witness cell Voc voltage after correction

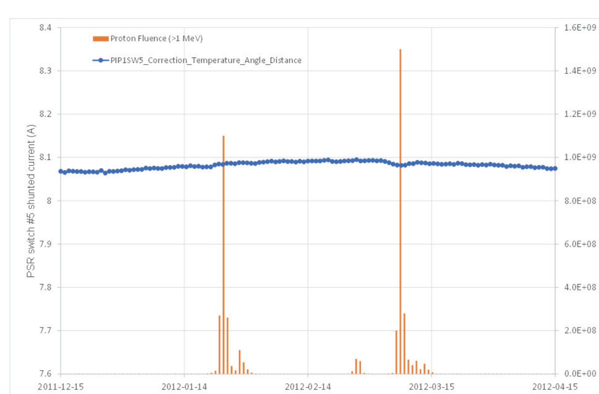

Fig. 14. Shunt switch Isc current after correction

Ⅳ. Conclusion

The Sun sometimes discharge large amount of energetic particles[7]. Even though a GEO orbit lies in the electron radiation belts, the protons from any solar event will still dominate the solar cell degradation[1]. Since COMS launch on June 26 2010, the proton events with the fluence of more than approximately 30 times the average level of perennial observations were observed between January 23-29 2012, and between March 07-14 2012 [16].

This paper studies the solar cell degradation by solar proton events in January and March 2012 for a witness cell Voc voltage and a shunt switch Isc current. The witness cell Voc voltage dropped about 23.6mV compare before the January 2012 proton events to after the March 2012 proton events. The Voc voltage dropped less than 1% at BOL, which is 2575mV. The shunt switch #5 Isc current decreased negligible, as expected, in the March 2012 proton events.

Reference

1) Messenger, S., Lorentzen, J. R., Walters, R. J., Warner, J. and Summers, G. P., "Electron to Proton Damage Correlation in Space Solar Cells," *IEEE 4th World Conference on Photovoltaic Energy*, 2006, pp. 1781~1784.

2) Lozinski, A. R., Horne, R. B., Glauert, S. A., Znna, G. D., Heyndericx, D. and Evans, H. D. R., "Solar Cell Degradation Due to Proton Belt Enhancements During Electric Orbit Raising to GEO," *Space Weather Research Article*, 2019, pp. 1059~1072.

3) Sarno-Smith, L. K., "A Radiation Belt MeV Electron Flux Comparison Between RBE and GOES-15," *Researchgate article*, April 2015.

4) ESTEC, *Space engineering - Space environment*, ECSS-E-10-04A, January 2000, p. 117.

5) Fortescue, P., Swinerd, G. and Stark, J., *Spacecraft System Engineering*, 4th Ed., John Wiley & Sons Ltd., 2011, pp. 25~31.

6) Messenger, S., Jackson, E. M., Warner, J. and Walters, R., "SCREAM: A New Code for Solar Cell Degradation Prediction using the Displacement Damage Approach," *IEEE 35th Photovoltaic Specialists Conference*, 2010, pp. 1106~1111.

7) Hu, S., "Solar Particle Events and Radiation Exposure in Space," *Researchgate article*, March 2017.

8) Rojdev, K., Tylka, A. J. and Atwell, W., "Preliminary Radiation Analysis of the Total Ionizing Dose for the Resource Prospector Mission," *AIAA*, August 2015.

9) ftp://ftp.swpc.noaa.gov/pub/indices/, accessed September 10, 2021.

10) https://www.swpc.noaa.gov/products/solar-cycle-progression, Data/Observed Solar Cycle Indices Data (JSON), accessed September 10, 2021.

11) ftp://ftp.swpc.noaa.gov/pub/warehouse/, accessed September 10, 2021.

12) Messenger, S. R., et al., "Correlation of Telemetered Solar Array Data with Particle Detector Data on GPS Spacecraft," *IEEE Transactions on Nuclear Science*, Vol. 58, No. 6, December 2011.

13) https://www.swpc.noaa.gov/sites/default/files/images/GOES%20Particles%20Improvements%20and%20Changes.pdf, GOES-16 Space Environment In-situ Sensor Suite Energetic Particle Measurements.

14) https://www.swpc.noaa.gov/content/space-weather-glossary.

15) Imaizumi, M., Nakamura, T., Takamoto, T., Ohshima, T. and Tajima, M., "Radiation Degradation Characteristics of Component Subcells in Inverted Metamorphic Triple-junction Solar Cells Irradiated with Electrons and Protons," *Progress in Photovoltaics: Research and Applications*, November 2016, pp. 161~174.

16) Nesterishin, M., et al., "Solar Cell Photochemical Contamination in MEO. Additional Evidence of Solar Array Non-radiation Degradation, based on Flight Data," *12th European Space Power Conference*, October 2019.

17) Duffie, J. A. and Beckman, W. A., *Solar Engineering of Thermal Processes*, 4th Ed., Wiley, 2013, pp. 5~20.

18) https://celestrak.com/columns/v04n09/, More on Geostationary Orbits, July 1998.